J Biomol NMR (2008) 40:65–70
DOI 10.1007/s10858-007-9209-z

ARTICLE

Probing the equilibrium unfolding of ketosteroid isomerase through xenon-perturbed $^{1}H–^{15}N$ multidimensional NMR spectroscopy

Hyeong Ju Lee · Hye Seon Moon · Do Soo Jang · Hyung Jin Cha · Bee Hak Hong · Kwan Yong Choi · Hee Cheon Lee

Received: 24 October 2007 / Accepted: 30 October 2007 / Published online: 15 November 2007

Abstract We used xenon-perturbed $^{1}H–^{15}N$ multidimensional NMR to investigate the structural changes in the urea-induced equilibrium unfolding of the dimeric ketosteroid isomerase (KSI) from *Pseudomonas putida* biotype B. Three limited regions located on the β3-, β5- and β6-strands of dimeric interface were significantly perturbed by urea in the early stage of KSI unfolding, which could lead to dissociation of the dimer into structured monomers at higher denaturant concentration as the interactions in these regions are weakened. The results indicate that the use of xenon as an indirect probe for multidimensional NMR can be a useful method for the equilibrium unfolding study of protein at residue level.

Keywords NMR · Ketosteroid isomerase · Equilibrium unfolding · Urea · Xenon · Dimeric protein

Introduction

Protein folding is an active and important research area in current structural biology (Miranker and Dobson 1996), and numerous studies on the folding pathways for a number of proteins have been performed by various experimental or theoretical methods. Equilibrium unfolding is one of the useful methods for the study of protein folding, since it can provide definite insights into protein stabilities and structural changes during unfolding of proteins. Thus, circular dichroism (CD) and fluorescence spectroscopy have been used to understand the global features of unfolding, in particular for the dimeric proteins (Gloss and Mathews 1997; Mallam and Jackson 2006; Zeeb et al. 2004), while NMR together with hydrogen exchange, relaxation and high-pressure studies have been used to obtain the unfolding characteristics at residue level (Burgering et al. 1995; Korzhnev et al. 2006; Kumar et al. 2006; Tang et al. 2006).

The use of small probe molecules designed to interact with target sites to describe them is an elegant approach, and xenon appears as a promising probe for NMR structural study of proteins because of its inertness to chemical reaction, binding preference to hydrophobic cavities and remarkable chemical shift sensitivity to non-bonded local environment (Quillin et al. 2000; Tilton et al. 1984). Thus, the existence of hydrophobic cavities has been detected in several proteins through the influence of xenon concentration on the protein ^{1}H and ^{15}N chemical shifts (Dubois et al. 2004; Gröger et al. 2003; Lowery et al. 2005). However, the possibility of using xenon as a means for studying the protein folding by multidimensional NMR has not been well tested until now, even though the hydrophobic regions in protein can be significantly disturbed during unfolding.

In this paper, we present new NMR approach for the equilibrium unfolding study of protein, in which xenon is employed as an indirect probe for multidimensional NMR to investigate the structural changes in the urea-induced equilibrium unfolding of ketosteroid isomerase (KSI) from *Pseudomonas putida* biotype B. KSI is a homodimeric

H. J. Lee · H. S. Moon · H. C. Lee (✉)
Department of Chemistry, Pohang University of Science and Technology, Pohang 790-784, Republic of Korea
e-mail: hcl@postech.ac.kr

D. S. Jang · H. J. Cha · B. H. Hong · K. Y. Choi
Division of Molecular Life Sciences, Pohang University of Science and Technology, Pohang 790-784, Republic of Korea

Present Address:
D. S. Jang
The J. David Gladstone Institute, San Fransico, CA 94158, USA

protein with six-stranded β-sheets and three α-helices in each cone-shaped monomer (131 amino acid residues per monomer), which catalyzes the allylic isomerization of a variety of Δ^5-3-ketosteroids by intramolecular transfer of the C4β proton to the C6β position (Ha et al. 2001; Pollack 2004; Pollack et al. 1999). Equilibrium unfolding studies on KSI by CD and fluorescence spectroscopy revealed that the protein followed a simple two state mechanism (Kim et al. 2001), while recent unfolding study by NMR and small angle X-ray scattering indicated the existence of a monomer-like intermediate during unfolding of KSI (Jang et al. 2006). Our results show that three limited regions located on the β3-, β5- and β6-strands of dimeric interface were significantly perturbed by urea in the early stage of KSI unfolding, suggesting that the unfolding process could begin at these regions with an increase of the denaturant concentration.

Materials and methods

Preparation of labeled KSI sample

Recombinant ^{15}N KSI was purified from *Escherichia coli* BL21 DE3 (Novagen Inc.) grown in 2 L of minimal medium (M9) containing ^{15}N ammonium chloride as the nitrogen source. The ^{13}C-, ^{15}N-, and ^{2}H labeled protein sample was overexpressed in the M9 medium containing ^{13}C glucose, ^{15}N ammonium chloride and D_2O, and purified as previously described (Kim et al. 2001). Homogeneity of KSI was confirmed by a single band in the PAGE analysis. ^{15}N-labeled KSI or triple-labeled KSI of ca. 1 mM was dissolved in 20 mM potassium phosphate buffer (pH 7.0, 10% v/v D_2O) with 1 mM dithiothreitol (DTT) and a small amount of sodium 2,2-dimethyl-2-silapentane-5-sulfonate (DSS) for internal chemical shift reference. Protein solutions with 3.5 and 4.5 M urea were prepared by dissolving KSI in the phosphate buffer described above with appropriate amounts of urea. Special NMR tube with a pressure valve (Wilmad, model 528-PV-7) was used to dissolve a definite amount of xenon (natural abundance) in the samples, and the xenon gas pressure of 8 atm was used for 2D HSQC experiments. To dissolve xenon gas as much as possible in the sample solution, the experimental step of degassing by weak decompression and purging xenon gas of ca. 4 atm was repeated for 3–4 times prior to pressurizing xenon gas with final pressure of 8 atm to the protein solution.

NMR experiments

NMR experiments for backbone assignments were performed at 298 K on a Bruker Avance 800 spectrometer (800.25 MHz for ^{1}H frequency; Korea Basic Science Institute at Ochang) equipped with a triple resonance probe and pulsed-field *x*-, *y*-, *z*-gradient capabilities. Sequence specific backbone assignments were obtained from the triple resonance experiments, HNCA, HN(CO)CA, HNCACB and HN(CO)CACB in TROSY type (Pervushin et al. 1997; Piotto et al. 1992; Sklenar et al. 1993). HNCA and HN(CO)CA spectra were recorded with 70 data points along t_1 domain, 48 data points along t_2 domain, and 1024 data points along t_3 domain. HNCACB and HN(CO)CACB spectra were recorded with 122 data points along t_1 domain, 48 data points along t_2 domain, and 1024 data points along t_3 domain. All 3D spectra were recorded using Echo-Antiecho method (Kay et al. 1992) in t_2 dimension, and States-TPPI method (Marion et al. 1989) in t_1 dimension with a relaxation delay of 1 s.

2D NMR experiments were performed at 298 K on a Bruker DRX 500 spectrometer (500.13 MHz for ^{1}H frequency) equipped with a broad-band inverse probe and pulsed-field *z*-gradient capability. ^{1}H-^{15}N TROSY-HSQC spectra were recorded with 256 data points along t_1 domain and 4096 complex data points along t_2 domain using States-TPPI method in t_1 dimension with a relaxation delay of 1 s. The ^{1}H chemical shifts were calibrated to DSS, and indirect referencing was used for the determination of ^{15}N chemical shifts (Wishart et al. 1995).

Results and discussion

Sequence specific backbone assignments for the native KSI and the protein with 3.5 M urea were carried out using the characteristic chemical shifts of the $^{13}C^{\alpha}$ of 13 glycines in HNCA spectra, $^{13}C^{\beta}$ of 12 alanines, 3 serines, 4 theronines, and 180 phase-shifted $^{13}C^{\alpha}$ of 13 glycines in HNCACB spectra as starting points (Zhao et al. 1997) as well as the general characteristics of HNCA and HNCACB experiments. A total of 110 and 107 residues were assigned for the native KSI and the protein with 3.5 M urea, respectively, and Fig. 1 shows the finger print ^{1}H-^{15}N HSQC spectra of both KSI samples. The resonances of the native KSI are shown in black, and those of KSI with 3.5 M urea are in red. As can be seen in Fig. 1, the ^{1}H–^{15}N HSQC spectrum of KSI with 3.5 M urea is almost identical to that of the native protein, indicating that the effect of 3.5 M urea on KSI is relatively small, leaving the protein largely unaffected. According to the equilibrium unfolding study on KSI by CD and fluorescence spectroscopy, the urea concentration of 3.5 M lies in the flat baseline region of the urea-induced transition curve (Kim et al. 2001).

^{1}H–^{15}N HSQC spectra were collected from the native KSI and the protein with 3.5 M and 4.5 M urea in the presence and absence of xenon. The ^{1}H and ^{15}N shift

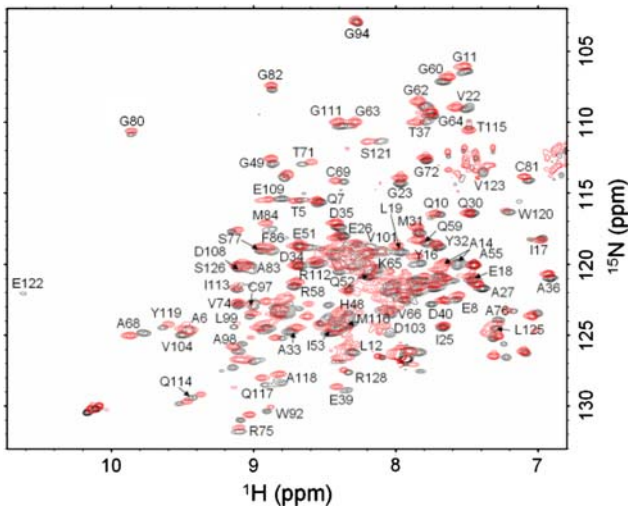

Fig. 1 Finger print ^{1}H–^{15}N HSQC spectra of KSI. The resonance of the native KSI are shown in black, and those of the protein with 3.5 M urea are in red. Some of the labels are not shown because of severe overlaps between resonances

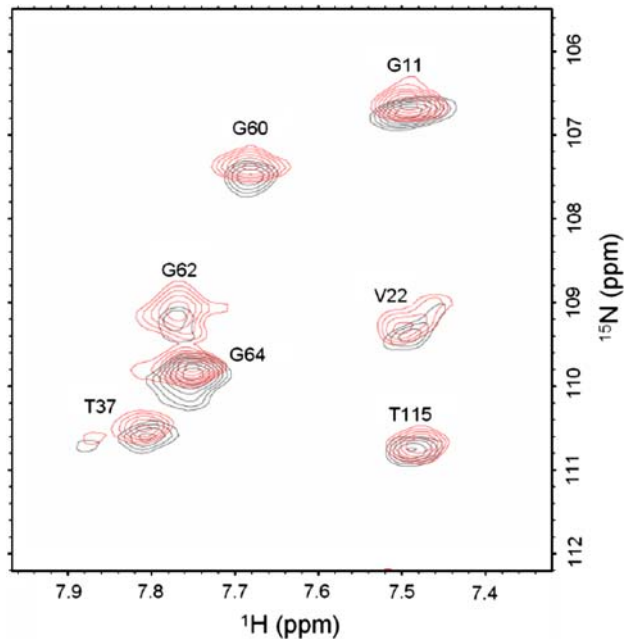

Fig. 2 Selected region from the ^{1}H–^{15}N HSQC spectrum of the native KSI. The resonance of the xenon-free KSI are shown in black, and those of KSI pressurized with xenon are in red

assignments for KSI with 4.5 M urea were obtained by comparing cross-peaks from the ^{1}H–^{15}N HSQC spectrum with those of KSI under 3.5 M urea condition. Figure 2 shows a selected region from the ^{1}H–^{15}N HSQC spectrum of the native KSI. The resonances of the xenon-free KSI are shown in black, and those of KSI pressurized with xenon are in red. As can be seen in Fig. 2, considerable signal shifts in the ^{1}H and ^{15}N dimension are induced by xenon for the native KSI. In order to quantitatively evaluate the shift of amide group cross-peaks in the ^{1}H–^{15}N HSQC spectra, the cumulative chemical shift changes ($\Delta\delta$) were determined for each of the residues according to the following equation:

$$\Delta\delta = \left[(\Delta\delta_H)^2 + (\Delta\delta_N)^2\right]^{1/2} \quad (1)$$

where $\Delta\delta_H$ and $\Delta\delta_N$ denote the xenon-induced chemical shifts measured in Hz in ^{1}H and ^{15}N dimension, respectively. The uncertainty in $\Delta\delta$ due to measurement errors was estimated to be about 2 Hz using three different data sets for the native KSI. Thus, any shift changes above 2 Hz could be considered to be real and significant.

Figure 3 shows the plot of the xenon-induced $\Delta\delta$ as a function of the amino acid residue number for the native KSI and the protein with 3.5 M and 4.5 M urea. The depicted secondary structures on top of the figure were assigned on the basis of previously reported crystal structure of KSI (Kim et al. 1997). Pressure-induced effects of xenon on the chemical shifts are known to be negligible (Gröger et al. 2003). Xenon is also very inert and has almost no effect on the protein structure (Rubin et al. 2001) or stabilization/destabilization (Tanner et al. 2001; Blobel et al. 2007). Furthermore, since the xenon-induced $\Delta\delta$ is obtained by a subtraction of the ^{1}H and ^{15}N chemical shifts with xenon from those without xenon at the same urea concentration, any effects of urea interaction with protein molecules on the chemical shifts should be cancelled. Thus, the observed signal shifts must be attributed to the interaction between protein molecules and dissolved xenon atoms. As can be seen in Fig. 3, it appears that the signal shifts vary along the sequence, and this must have bearing on the different interactions of the xenon along the polypeptide chain. The average $\Delta\delta$ amounts to relatively small value of 3–4 Hz for all KSI samples, which is expected for nonspecific interaction of xenon with hydrophobic surface patches of protein (Dubois et al. 2004; Gröger et al. 2003). For specific xenon-protein interaction, the xenon-induced shifts were reported to be ca. 40–50 Hz (Dubois et al. 2004; Gröger et al. 2003; Lowery et al. 2005; Rubin et al. 2002). Besides the graphs in Fig. 3, solid ribbon diagrams coded by the values of $\Delta\delta$ are presented to show the trends of xenon-induced shifts more clearly, where the $\Delta\delta$ values beyond a specific cut-off are marked by black (over the sum of average and standard deviation), dark gray (over average), light gray (below average), and white (no data). It can bee seen from the diagrams that the residues perturbed most significantly by xenon are concentrated on a broad region around the dimeric interface. The clusters of residues largely perturbed by xenon did not show good correlations with 16 hydrophobic pockets searched by the CASTp software (Binkowski et al. 2003) for KSI wild-type monomer (PDB ID: 1OPY), suggesting that xenon interacts with KSI in a nonspecific manner.

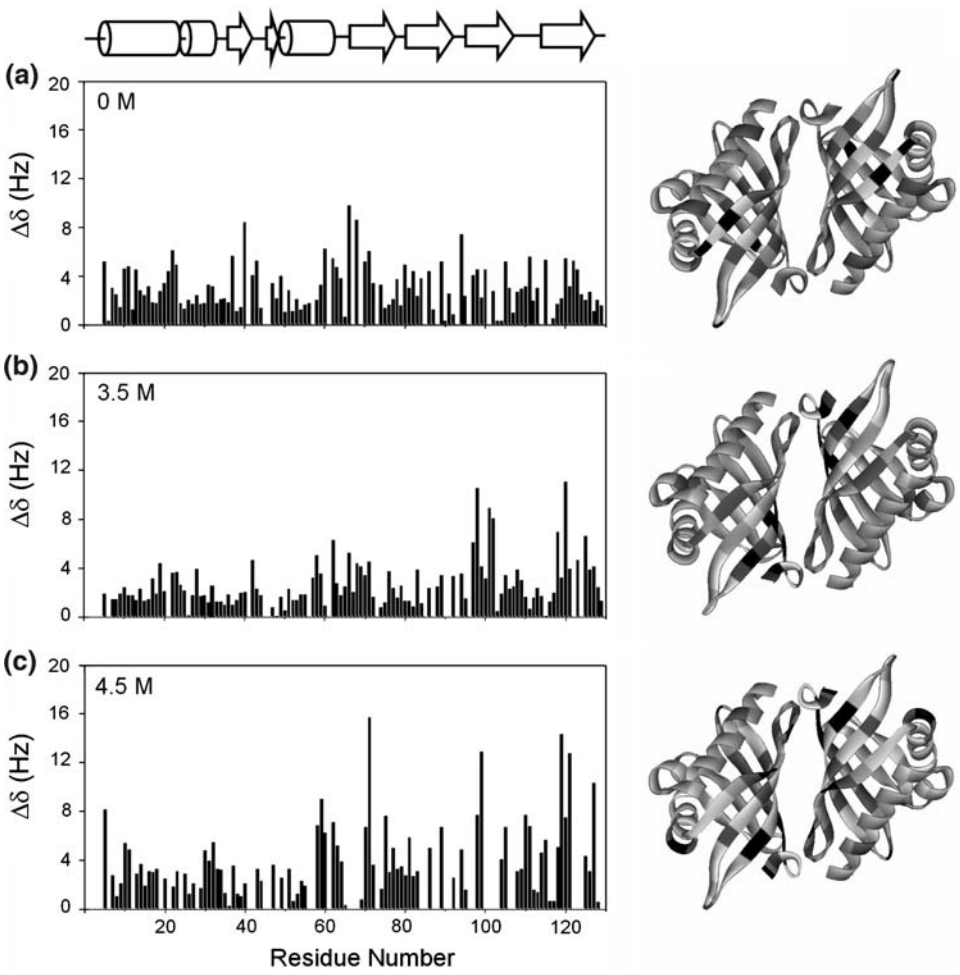

Fig. 3 Plot of the xenon-induced cumulative chemical shift changes ($\Delta\delta$ given by Eq. 1 in the text) as a function of the amino acid residue number for (**a**) the native KSI, (**b**) KSI with 3.5 M urea and (**c**) KSI with 4.5 M urea. The secondary structure elements are depicted on top of the figure; α-helices are marked with cylinders, and β-strands are marked with arrows. Besides the graphs, solid ribbon diagrams coded by the values of $\Delta\delta$ are presented, where the $\Delta\delta$ values beyond a specific cut-off are marked by black (over the sum of average and standard deviation), dark gray (*over average*), light gray (*below average*), and white (*no data*)

In order to understand the effects of urea on the structural characteristics of KSI more definitely, the differences in the xenon-induced $\Delta\delta$ between the native KSI and the protein with 3.5 M urea ($\Delta\Delta\delta = \Delta\delta_{0M} - \Delta\delta_{3.5M}$) were calculated as shown in Fig. 4a. The $\Delta\delta$ values for KSI with 3.5 M urea are in general slightly smaller than those for the native KSI, presumably due to the interference of denaturant molecules with easy access of xenon to protein surfaces. Nevertheless, two limited regions (residues 97–108 and 117–127 that belong to β5- and β6-strands, respectively) are more significantly perturbed by the presence of xenon under 3.5 M urea condition than the native KSI, which correspond to the negative histograms in Fig. 4a. Such differences in $\Delta\delta$ between the two states of KSI could be attributed to urea-induced local perturbations in the tertiary structure of the protein. Thus, it seems that the region formed mainly by the β5- and β6-strands is more vulnerable to structural perturbations by urea than other regions, which would make the two strands more exposed to xenon under 3.5 M urea condition.

We now show in Fig. 4b the differences in $\Delta\delta$ between the native KSI and the protein with 4.5 M urea ($\Delta\Delta\delta = \Delta\delta_{0M} - \Delta\delta_{4.5M}$). As the urea concentration increases from 3.5 M to 4.5 M, additional region (residues 69–77 that belong to β3-strand) is significantly perturbed by urea, while the existing perturbations in β5- and β6-strands become even stronger, indicating a stepwise enhancement of structural changes with the increase of denaturant concentration. Since the β3-, β5- and β6-strands constitute the dimeric interface of KSI together with the β4-strand, it seems that the interface region of the protein is significantly perturbed by urea during early stage of KSI unfolding, which could lead to dissociation of the dimer into structured monomers at higher denaturant concentration. Furthermore, the interactions around the β5- and β6-strands appear to be weakened first in the unfolding process by urea, suggesting that the unfolding of KSI might begin at this region of two strands. The results are consistent with those of our previous study on the size of KSI during urea-induced unfolding (Jang et al. 2006), where NMR and small angle X-ray scattering measurements consistently indicated the existence of a compact monomer-like intermediate at the urea concentration of 5.2 M.

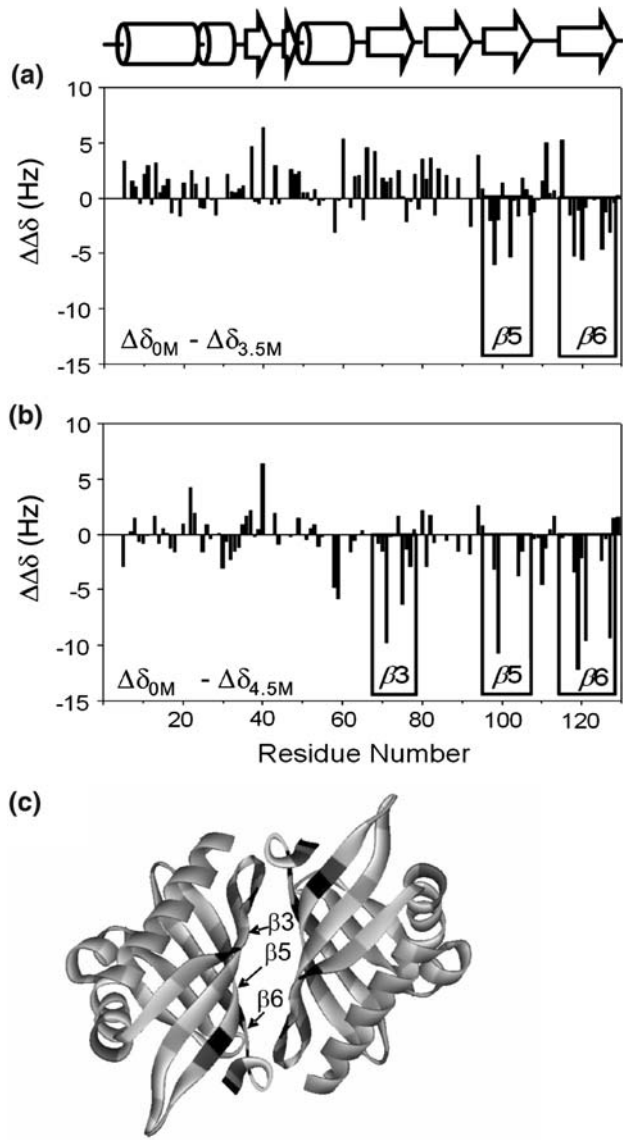

Fig. 4 Differences ($\Delta\Delta\delta$) in the xenon-induced cumulative chemical shift changes. (**a**) Plot of $\Delta\Delta\delta$ between the native KSI and the protein with 3.5 M urea ($\Delta\Delta\delta = \Delta\delta_{0M} - \Delta\delta_{3.5M}$) as a function of the amino acid residue number. (**b**) Plot of $\Delta\Delta\delta$ between the native KSI and the protein with 4.5 M urea ($\Delta\Delta\delta = \Delta\delta_{0M} - \Delta\delta_{4.5M}$) as a function of the amino acid residue number. (**c**) Solid ribbon diagram coded by the values of $\Delta\Delta\delta$ from the plot in (**b**). The residues with large negative $\Delta\Delta\delta$ values beyond a specific cut-off (sum of average and standard deviation) are shown in black, the residues with no data in white, and the rest of the residues having small $\Delta\Delta\delta$ values in either dark or light gray

Figure 4c is a solid ribbon diagram coded by the values of $\Delta\Delta\delta$ in Fig. 4b, where the residues with large negative $\Delta\Delta\delta$ values beyond a specific cut-off (ca. -6 Hz, sum of average and standard deviation) are shown in black. The residues that are excluded from the analysis due to lack of peak assignments in either xenon-free or xenon-added KSI are shown in white, while the rest of the residues having relatively small $\Delta\Delta\delta$ values are in either dark (above average) or light (below average) gray. As can be seen in Fig. 4c, it is clear again that the most significantly perturbed residues by urea are mainly located on the dimeric interface region of KSI.

In conclusion, we have investigated the effects of urea on the structural changes in the equilibrium unfolding of KSI by using xenon-based multidimensional NMR spectroscopy. Our results clearly demonstrate that the subtle structural changes in the early stage of protein unfolding can be easily monitored at amino acid resolution by multidimensional NMR with the use of xenon as an indirect probe, and suggest that this new NMR approach can be a useful method for the equilibrium unfolding study of protein.

Acknowledgements This work was supported by the grant from Korea Research Foundation (C00178). One of the authors (H.J.L) thanks Dr. Sung Jin Park and Dr. Woo Sung Son at National Research Laboratory of Membrane Protein Structure in Seoul National University for helpful discussion in backbone assignments.

References

Binkowski TA, Naghibzadeh S, Liang J (2003) CASTp: computed atlas of surface topography of proteins. Nucleic Acids Res 31:3352–3355

Blobel J, Schmidl S, Vidal D, Nisius L, Bernado P, Millet O, Brunner E, Pons M (2007) Protein tyrosine phosphatase oligomerization studied by a combination of ^{15}N NMR relaxation and ^{129}Xe NMR. Effect of buffer containing arginine and glutamic acid. J Am Chem Soc 129:5946–5953

Burgering MJ, Hald M, Boelens R, Breg JN, Kaptein R (1995) Hydrogen exchange studies of the Arc repressor: evidence for a monomeric folding intermediate. Biopolymers 35:217–226

Dubois L, Da Silva P, Landon C, Huber JG, Ponchet M, Vovelle F, Berthault P, Desvaux H (2004) Probing the hydrophobic cavity of lipid transfer protein from *Nicotiana tabacum* through xenon-based NMR spectroscopy. J Am Chem Soc 126:15738–15746

Gloss LM, Mathews CR (1997) Urea and thermal equilibrium denaturation studies on the dimerization domain of *Escherichia coli* Trp repressor. Biochemistry 36:5612–5623

Gröger C, Moglich A, Pons M, Koch B, Hengstenberg W, Kalbitzer HR, Brunner E (2003) NMR-spectroscopic mapping of an engineered cavity in the I14A mutant of HPr from *Staphylococcus carnosus* using xenon. J Am Chem Soc 125:8726–8727

Ha NC, Choi G, Choi KY, Oh BH (2001) Structure and enzymology of Δ^5-3-ketosteroid isomerase. Curr Opin Struct Biol 11:674–678

Jang DS, Lee HJ, Lee B, Hong BH, Cha HJ, Yoon J, Lim K, Yoon YJ, Kim J, Ree M, Lee HC, Choi KY (2006) Detection of an intermediate during the unfolding process of the dimeric ketosteroid isomerase. FEBS Lett 580:4166–4171

Kay LE, Keifer P, Saarinen T (1992) Pure absorption gradient enhanced heteronuclear single quantum correlation spectroscopy with improved sensitivity. J Am Chem Soc 114:10663–10665

Kim DH, Nam GH, Jang DS, Yun S, Choi G, Lee HC, Choi KY (2001) Roles of dimerization in folding and stability of ketosteroid isomerase from *Pseudomonas putida* biotype B. Protein Sci 10:741–752

Kim SW, Cha SS, Cho HS, Kim JS, Ha NC, Cho MJ, Joo S, Kim KK, Choi KY, Oh BH (1997) High-resolution crystal structures of Δ^5-3-ketosteroid isomerase with and without a reaction intermediate analogue. Biochemistry 36:14030–14036

Korzhnev DM, Bezsonova I, Evanics F, Taulier N, Zhou Z, Bai Y, Chalikian TV, Prosser RS, Kay LE (2006) Probing the transition state ensemble of a protein folding reaction by pressure-dependent NMR relaxation dispersion. J Am Chem Soc 128:5262–5269

Kumar A, Srivastava S, Kumar Mishra R, Mittal R, Hosur RV (2006) Residue-level NMR view of the urea-driven equilibrium folding transition of SUMO-1 (1–97): native preferences do not increase monotonously. J Mol Biol 361:180–194

Lowery TJ, Doucleff M, Ruiz EJ, Rubin SM, Pines A, Wemmer DE (2005) Distinguishing multiple Chemotaxis Y protein conformations with laser-polarized 129Xe NMR. Protein Sci 14:848–855

Mallam AL, Jackson SE (2006) Probing nature's knots: the folding pathway of a knotted homodimeric protein. J Mol Biol 359:1420–1436

Marion D, Driscoll PC, Kay LE, Wingfield PT, Bax A, Gronenborn AM, Clore GM (1989) Overcoming the overlap problem in the assignment of ^{1}H NMR spectra of larger proteins by use of three-dimensional heteronuclear ^{1}H-^{15}N Hartmann-Hahn-multiple quantum coherence and nuclear Overhauser-multiple quantum coherence spectroscopy: application to interleukin 1β. Biochemistry 28:6150–6156

Miranker AD, Dobson CM (1996) Collapse and cooperativity in protein folding. Curr Opin Struct Biol 6:31–42

Pervushin K, Riek R, Wider G, Wuthrich K (1997) Attenuated T_2 relaxation by mutual cancellation of dipole–dipole coupling and chemical shift anisotropy indicates an avenue to NMR structures of very large biological macromolecules in solution Proc Natl Acad Sci USA 94:12366–12371

Piotto M, Saudek V, Sklenar V (1992) Gradient-tailored excitation for single-quantum NMR spectroscopy of aqueous solutions. J Biomol NMR 2:661–665

Pollack RM (2004) Enzymatic mechanisms for catalysis of enolization: ketosteroid isomerase. Bioorg Chem 32:341–353

Pollack RM, Thornburg LD, Wu ZR, Summers MF (1999) Mechanistic insights from the three-dimensional structure of 3-oxo-Δ^5-steroid isomerase. Arch Biochem Biophys 370:9–15

Quillin ML, Breyer WA, Griswold IJ, Matthews BW (2000) Size versus polarizability in protein-ligand interactions: binding of noble gases within engineered cavities in phage T4 lysozyme. J Mol Biol 302:955–977

Rubin SM, Lee SY, Ruiz EJ, Pines A, Wemmer DE (2002) Detection and characterization of xenon-binding sites in proteins by ^{129}Xe NMR spectroscopy. J Mol Biol 322:425–440

Rubin SM, Spence MM, Dimitrov IE, Ruiz EJ, Pines A, Wemmer DE (2001) Detection of a conformational change in maltose binding protein by ^{129}Xe NMR spectroscopy. J Am Chem Soc 123:8616–8617

Sklenar V, Piotto M, Leppik R, Saudek V (1993) Gradient-tailored water suppression for ^{1}H-^{15}N HSQC experiments optimized to retain full sensitivity. J Magn Reson A 102:241–245

Tang Y, Grey MJ, McKnight J, Palmer AG 3rd, Raleigh DP (2006) Multistate folding of the villin headpiece domain. J Mol Biol 355:1066–1077

Tanner JW, Johansson JS, Liebman PA, Eckenhoff RG (2001) Predictability of weak binding from X-ray crystallography: inhaled anesthetics and myoglobin. Biochemistry 40:5075–5080

Tilton RF Jr, Kuntz ID Jr, Petsko GA (1984) Cavities in proteins: structure of a metmyoglobin-xenon complex solved to 1.9 Å. Biochemistry 23:2849–2857

Wishart DS, Bigam CG, Yao J, Abildgaard F, Dyson HJ, Oldfield E, Markley JL, Sykes BD (1995) ^{1}H, ^{13}C and ^{15}N chemical shift referencing in biomolecular NMR. J Biomol NMR 6:135–140

Zeeb M, Lipps G, Lilie H, Balbach J (2004) Folding and association of an extremely stable dimeric protein from *Sulfolobus islandicus*. J Mol Biol 336:227–240

Zhao Q, Abeygunawardana C, Mildvan AS (1997) NMR studies of the secondary structure in solution and the steroid binding site of Δ^5-3-ketosteroid isomerase in complexes with diamagnetic and paramagnetic steroids. Biochemistry 36:3458–3472